

REGISTRATION OF UNRECTIFIED OPTICAL AND SAR IMAGERY OVER MOUNTAINOUS AREAS THROUGH AUTOMATIC FREE-FORM FEATURES GLOBAL MATCHING

D. I. Vassilaki ^a, Ch. C. Ioannidis ^a, A. A. Stamos ^b

^a School of Rural and Surveying Engineering, ^b School of Civil Engineering
National Technical University of Athens, 9 Iroon Polytechniou Str, 15780 Zografos, Greece –
dimitra.vassilaki@gmail.com, cioannid@survey.ntua.gr, stamthan@central.ntua.gr

Commission I, WG I/2, I/4

KEY WORDS: Automation, Matching, Registration, Algorithms, SAR, Optical, TerraSAR-X

ABSTRACT:

An algorithm, for automatic global matching of heterogeneous free-form features (natural features) between the 3dimensional object space and the 2dimensional image space, taking into account the non-rigid nature of the projection transformation is presented in this paper. The proposed algorithm is based on the the well-known Iterative Closest Point (ICP) algorithm. The algorithm is tested for the registration of high resolution TerraSAR-X and optical imagery of a mountainous site in the North East of Athens. The registration is based on free-form road centerline matching. Ground Control Features (GCFs) and DTM information is obtained from old existing maps of the area, while road centerlines are calculated from road edges using skeletonization techniques. The rectification is done with standard techniques and the results are encouraging.

1. INTRODUCTION

Recent advances in SAR sensors, such as the unprecedented resolution of TerraSAR's and COSMO-SkyMed's sensors, have conceptualized the complementary use of optical and SAR satellite data. SAR and optical data present many differences and similarities simultaneously. Although, in the past, the similarities led to the competition for the exclusive use of SAR or optical data, today their differences, and thus their mutual usefulness and effectiveness are fully appreciated. The concept of complimentary use of SAR and optical data is illustrated by the cooperation of optical and SAR satellites, (e.g. CNES/ASI Orfeo program), by the installation of both optical and SAR sensors on the same satellite (e.g. ALOS system), as well as by the compilation of scientific studies which end up in some specific applications of their combined use (Bellman and Hellwich, 2006; Raouf and Lichtenegger, 1997; Crosetto, 1998; Honikel, 1998; Karkee et al, 2006; Tupin, 2006; Sorgel et al, 2007; Orsomando et al, 2007; Wegner et al, 2008).

SAR and optical data registration is a prerequisite procedure of significant importance in many applications, such as image fusion, stereo formation and change detection. Although a lot of work has been done in the field of image registration (Zitova and Flusser, 2003), it remains an active field of research, especially for multimodal and multitemporal cases (Inglada and Giros, 2003), as the ones examined in this paper.

The new generation of spaceborne sensors, described before, offers the capability of the identification of terrain features, such as roads' surfaces, especially paved ones (Eineder et al, 2009), that was impossible to distinguish with sensors of the previous generation.

Feature Based Photogrammetry (FBP) states that linear features exhibit certain advantages over the classical, point based, approach for the orientation processes. Major advantages of linear features against points are (Mikhail, 1993; Zalmanson, 2000; Habib and Kelley, 2001; Akav et al, 2004; Wang et al, 2008):

- i. Man made and physical environment is rich of linear features (roads, pipelines, coastlines).
- ii. Linear features can be detected more reliably.
- iii. The matching of linear features is more reliable.
- iv. Linear features consist a continuous control of information.
- v. The identification of common linear features is more robust than node identification in multimodal and multitemporal registration, because experience tells that identification of common nodes is difficult and rare, and when a common pair of nodes is found (for example a crossroad), their exact relative position is often questionable.

This paper focuses on the joint use of optical and SAR images, and takes advantage of the linear features and the high resolution of the new space-borne SAR sensors. A feature-based matching method for the registration of unrectified optical and SAR images is presented. Applications were made on mountainous areas, which are not thoroughly investigated so far.

The method is based on the Iterative Closest Point (ICP), and matches heterogeneous free-form features (natural features) from the 3dimensional object space to the 2dimensional image space. In order to converge, the ICP needs a good first approximation which weakens its practicality, or at least it makes it awkward to use, as a first approximation must be given to the method manually. In this paper a method for the

automated computation of a good first approximation for ICP (2D-3D matching) is also presented.

The philosophy of the method, ignoring temporarily the algorithmic implementation, is that the microwave nature of SAR sensors in combination with the side-looking geometry, makes the identification of homologous free-form features much easier and less ambiguous, than the identification of salient point features, which are traditionally used for georeference and registration procedures. And that the same Ground Control Information is used for the georeference of SAR images and the georeference of the optical images, which leads to better co-registration of the images and less time and cost for the procedure.

2. PROPOSED METHOD

2.1 Problem Formulation

In this paper, the curves are considered as independent collections of consecutive nodes which are joined with straight line segments, or some other interpolation function such as cubic splines. In any case the original measurements, or information, is in the form of 2D or 3D node coordinates: $N_i(x_i, y_i)$, $N_i(x_i, y_i, z_i)$. This representation of curves is preferred, because the curves we are trying to match are free-form curves (natural curves) which represent objects of unknown geometry that appear in man-made environment, such as road centerlines, breaklines and contour lines. Alternatively if in some cases such as highway centerlines, the curves are analytic, the "interpolation" is done with the analytic curve itself. It is assumed that curves have been extracted from different kind of data and with different procedures, so they do not consist of corresponding nodes (number and position), as presented in fig. 1.

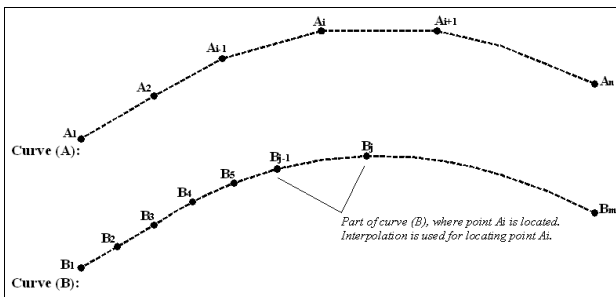


Figure 1. Example of heterogeneous free-form features.

The 2D transformations, such as similarity, which have been used to register SAR with optical images, show generally poor results in mountainous terrain, since they can not counter the geometric distortions due to arbitrary terrain. Even for flat, or at least plane terrain, the similarity transformation can not counter the systematic nonlinear sensor distortions (slant range), especially as the distortions of SAR sensors (cone/spherical projection) are very different to the distortions of optical sensors (central projection).

2.2 Overview of the proposed approach

Rigorous 3D to 2D projections that automatically take into consideration arbitrary terrain, are used. The projections are of

the form of polynomials or RPFs which take sensor distortions into account. Both images are rectified using the computed projections and the known DTM. Because the form of the projection is the same for both images, the coefficients of the projections are computed using the continuous information of the same linear feature, and the rectification is done with the same DTM, the geometric difference or error of the rectified images with respect to each other is minimized. Also, because the same computational procedures are used independently for both images, the time and the cost of the whole process are also minimized.

The presented method is based on the ICP algorithm. The ICP algorithm is a general purpose method for efficient registration of 2-D or 3-D shapes, including free-form curves and surfaces. The algorithm consists of four steps which are repeated until convergence within a tolerance (Besl and McKay, 1992; Zhang, 1994):

- i. Compute the closest points.
- ii. Compute the registration.
- iii. Apply the registration.
- iv. Check the threshold.

In the following paragraphs, issues concerning the steps of the ICP algorithm for the free-form curves matching are commented.

2.3 Closest Points Pairs between 2D Curves

In order to find the closest points between 2D curves, the second curve B (fig. 1) is split to a large set of consecutive interpolated points, each one very close to its previous and its next point. Then, the distances of all these points to a node of the first curve A may be computed, and the point with the least distance is the closest point to the node. For this brute-force method to produce good results, the distance between two consecutive interpolated points must be very small, which leads to a large set of points and large computation time. It is, however, relatively easy to speed up the process using the divide and conquer technique. The second curve B is split to a moderate number of points. The closest point to a node on the first curve A is located as described. Then the distance between the previous and next point of the closest is split to a finer mesh and a new closest point is located. The process is repeated until the interpolation distance is small enough.

More details can be found in (Vassilaki et al, 2008a) and in (Stamos et al, 2009) where parallel implementation is also considered.

2.4 Closest Points Pairs between a 3D and a 2D Curve

In the case examined in this paper, a 3D curve in object space is projected in the 2D image space using a projection transformation. This is a key issue in the computation of the closest points pairs between curves of different dimensionality. The algorithm begins with an approximation of the projection equation, which is computed automatically as described later. The nodes B_i of the 3D curve are projected to 2 dimensional nodes B'_i keeping into account the one-to-one relationship between B_i and B'_i (fig. 1). The nodes B'_i are matched to their closest points P_i of curve A using the algorithm of paragraph 2.3. Thus 3D node B_i which is projected to 2 dimensional node B'_i , is matched to 2D point P_i of curve A. Using the B_i , P_i pairs a new and improved approximation of the projection

equation may be computed, and the procedure is repeated until convergence. More details can be found in (Vassilaki et al, 2008b).

2.5 Automated Pre-alignment of the Curves

In order to converge, the ICP needs a good first approximation of the projection transformation. For estimating such an approximation, it is assumed that the orbits' elevations of both the optical and the SAR sensors are considerably high, so that the distortions due to sensor and the deformations due to terrain are comparatively small. Thus, the X, Y coordinates of a 3D feature (the Z coordinate is discarded) can be considered as a good approximation of the 2D projected coordinates, after being scaled to match the size of the SAR or optical image and, almost certainly, translated and rotated. The computation of the (best) similarity transformation between two 2-dimensional curves is briefly described below (Vassilaki et al, 2008c). The similarity transformation consists of a transfer, a rotation and a scale adjustment between the two curves, each one of which is approximated by a different method.

The vector difference of the centroids of the two curves are used as robust first approximation of the translations. The centroids are calculated as the mean of a large number of interpolated points of each curve.

The ratio of the lengths of the two curves is used as robust first approximation of the scale. The lengths are calculated as the cumulative distance of a large number of interpolated points of each curve.

For the estimation of the rotation three different approaches may be used:

- The average difference of the azimuths of characteristic points (first and last points of the curves) with respect to the common centroid. Theoretically the approach is not very robust as it depends on single nodes which, by chance, may contain bigger error than the rest of the nodes.
- The difference of the mean azimuths of the curves with respect to the common centroid, which are calculated indirectly through unit vectors. The approach gives poor results if the curves are nearly closed or nearly straight lines.
- A sequence of all possible rotations with $\Delta\phi$ step are tried and the one which gives the smallest ICP error is selected. The approach is robust but computationally intensive.

2.6 Transformation models

A number of projection transformation types were investigated:

- Polynomial projection of 1st order (3D affine transformation). Eight parameters define the relationship between the object space and the image space.

$$x = a1X + a2Y + a3Z + a4$$

$$y = b1X + b2Y + b3Z + b4$$

- Rational Polynomial Function of 1st order with common denominator (Direct Linear Transformation - DLT), with eleven parameters.

$$x = \frac{(a1X + a2Y + a3Z + a4)}{(c1X + c2Y + c3Z + 1)}$$

$$y = \frac{(b1X + b2Y + b3Z + b4)}{(c1X + c2Y + c3Z + 1)}$$

- Rational Polynomial Function of 1st order (RPF), with fourteen parameters.

$$x = \frac{(a1X + a2Y + a3Z + a4)}{(c1X + c2Y + c3Z + 1)}$$

$$y = \frac{(b1X + b2Y + b3Z + b4)}{(d1X + d2Y + d3Z + 1)}$$

It must be noted that the 1st order polynomial is the most stable projection, and the ICP always converges using it. However, the ICP using the 1st order RPF, sometimes fails to converge when the similarity is used as the first approximation. In order to achieve convergence, the 1st order polynomial is computed, and then this is used as a better first approximation for the higher order projections.

2.7 Workflow

The procedure of the method as described above may be summarized as follows:

- Compute first approximation of the projection.
- Project 3D curve to 2D remembering the relationship between 3D points and 2D points.
- Compute closest point pairs between projected curve and image curve.
- Using the relationship of step ii, produce point pairs between 3D curve and image curve.
- Compute improved projection from pairs.
- Repeat steps ii-v until convergence.

The proposed method was implemented in Fortran 95. For efficiency, convenience and user-friendliness, it was integrated with ThanCad (Stamos, 2007), which is a free/open source CAD.

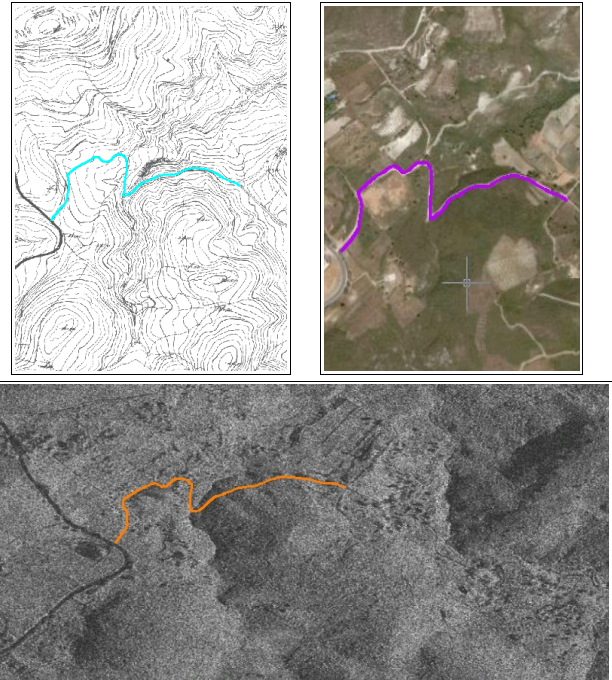


Figure 2. Topographic map (top left), optical image (top right) and SAR image (bottom).

3. APPLICATION TESTS

3.1 Test Area

The proposed method was tested using:

- a High Resolution SpotLight TerraSAR-X image
- an optical image downloaded from Google Earth
- a 40 years old topographic map

The SAR image was captured on February 2nd, 2009, it belongs to the School of Rural and Surveying Engineering of National Technical University of Athens and it was provided to the Lab. of Photogrammetry for the needs of this research. The range resolution is 0.45 m and the azimuth line resolution is 0.87 m. The optical image was captured by DigitalGlobe and was downloaded from Google Earth. The 40 years old map is of medium scale (1:5,000).

The application area is in the greater north-eastern region of Athens, Greece, and it has steep mountainous terrain of mean elevation of 270 m (fig. 2).

3.2 Preprocessing

TerraSAR's datafile (xml, cos) was converted to common standard format TIF using software ERDAS v9.3. The GDAL library could be used for the same job. The SAR image was converted to intensity, while keeping the slant range geometry of the original image. Then the image was flipped horizontally because it was the mirror of the optical image. No conversion was done to the optical image. The map was scanned with 400 dpi resolution and it was imported to CAD software, where it was corrected from the errors due to the contractions/expansions of the paper medium, and it was transformed to the new national geodetic reference system.

The road which was used as a linear feature of the matching, is shown in fig.3-fig.5. The road edges extraction was done manually, by digitizing the lines appeared on the data. The road centerline was obtained from the edges using skeletonization techniques (fig.3, fig.4, fig.5). The length of the road is about 950 m. The road centerline is preferred to road edges as control curve, because it has less error than the edges and it fully represents the geometry of the road.

The contour lines of the map, were digitized and converted to Triangulated Irregular Network (TIN) via Delaunay triangulation, which was used for the rectification. The TIN was also used as DTM in order to extract elevation information of the road.

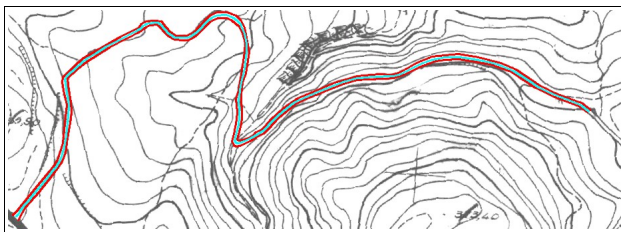


Figure 3. Map: road edges (lines in red), road centerline (in cyan).



Figure 4. Optical: road edges (lines in green), road centerline (in magenta).

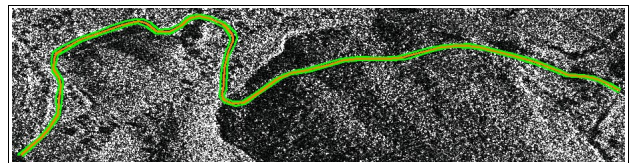


Figure 5. SAR image: road edges (line in green), road centerline (in orange).

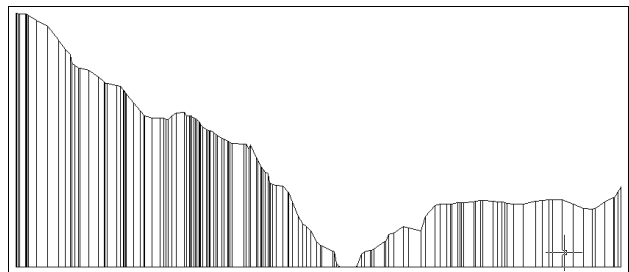


Figure 6. Profile of road centerline, computed by the DTM.

The rough profile of the road centerline is due to the small scale of the map and the fact that the map does not have elevation information along the surface of the road. The centerline elevation was computed by the surrounding terrain (fig.3, fig.6)

3.3 Rectification

The rectification of both images was done using standard procedures of orthophoto production. The necessary TIN was obtained by the map digitizing the contour lines. The type of the projection used for the rectification of both images was Rational Polynomial function of 1st order (RPF).

3.4 Work flow of the test

The computational steps taken for the test may be summarized as follows:

- i. Preprocessing (SAR, map).
- ii. Extraction of road edges (SAR, optical, map).
- iii. Calculation of road centerline (SAR, optical, map).
- iv. SAR to map matching, using 3D road centerline and its 2D projection.
- v. SAR rectification, using the TIN obtained by the map and the projection computed in step iv.
- vi. Optical to map matching, using 3D road centerline and its 2D projection.
- vii. Optical rectification, using the TIN obtained by the map and the projection computed in step vi.
- viii. SAR to optical overlay, for illustration purposes.

3.5 Results

The results of the matching are shown in fig. 7, for the optical image and in fig. 8, for the SAR image. For illustration purposes the initial curves are shown together, though in reality their coordinates are completely unrelated. The figures show the 3D curve from map (cyan), the 2D curve from SAR/optical (red), the first approximation (blue dashed), the matched 3D curve to 2D using similarity transformation (light blue dashed dot), the matched 3D curve to 2D using 1st order Rational Polynomial Projection (black).

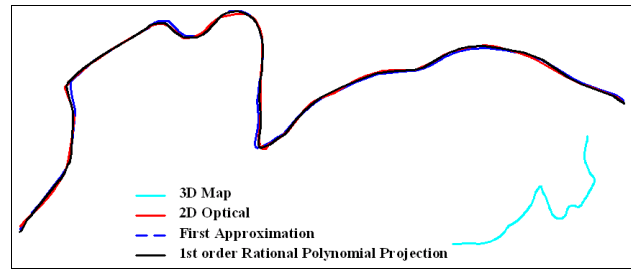


Figure 7. Matching results: Optical image to Map.

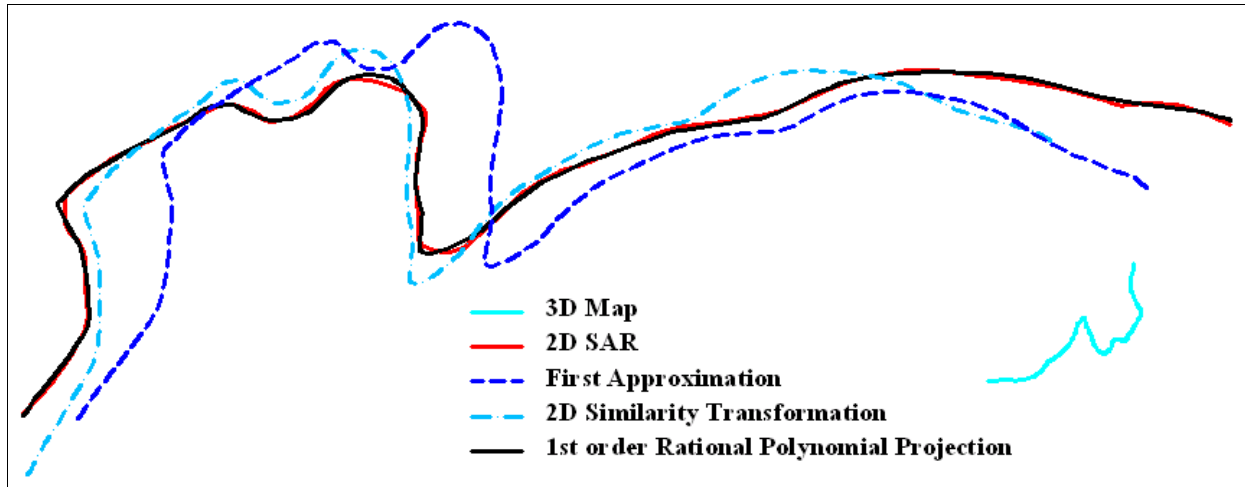


Figure 8. Matching results: SAR image to Map.

As shown in Figure 8 the matching of the curves is successful. The rms error between the matched curves is shown in Table 9 for various projection types. The achieved matching accuracy is satisfactory, considering that the horizontal and vertical accuracy of the topographic map is of 1.5 m and 2 m respectively. A combination of the rectified images are shown in Figure 10.

Transformation/ Projection	SAR to Map	Optical to Map
	rms (m)	rms (m)
1 st approximation	13.61	3.20
2D Similarity	8.15	2.29
1 st order Polynomial	1.61	1.49
DLT	1.42	1.39
1 st order RPF	1.39	1.08

Table 9. Matching results

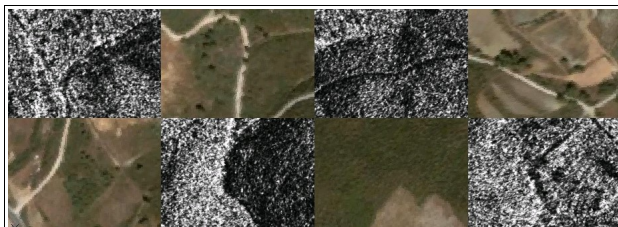


Figure 10. Registration results: Optical to SAR.

4. CONCLUSIONS

In this paper, a method for automatic global matching of heterogeneous free-form linear features between the 3dimensional object space and the 2dimensional image space was presented. The method is based on ICP and handles any non-rigid projection type. The method uses linear features which are much easier to locate and more robust than salient points, especially for the speckled SAR images. The method produces very good results, as was illustrated in a typical mountainous site of Greece.

For further work, the expansion of the proposed method for matching networks of free form curves can be investigated, as a curve may be confined to a small region of the image leading to a registration not representative of the whole image.

REFERENCES

- Akav, A., Zalmanson, G.H. and Doytsher, Y., 2004. Linear Feature Based Aerial Triangulation. In: International Archives of Photogrammetry and Remote Sensing, Vol XXXV.
- Bellman, A. and Hellwich, O., 2006. Sensor and Data Fusion Contest: Information for Mapping from Airborne SAR and Optical Imagery (Phase 1). *EuroSDR Projects, Official Publication No. 50*, Frankfurt, Germany.
- Besl, P.J. and McKay, N.D., 1992. A Method for Registration of 3-D Shapes. *IEEE Transactions on Pattern Analysis and Machine Intelligence*, 14(2), pp. 239-256.

- Crosetto, M., 1998. Interferometric SAR for DEM Generation: Validation of an Integrated Procedure Based on Multisource Data. *Doctorate thesis*, Politecnico di Milano, Geodetic and Surveying Sciences, Milano, Italy.
- Eineder, M., Adam, N., Bamler, R., Yaque-Martinez, N., Breit, H., 2009. Spaceborne Spotlight SAR Interferometry with TerraSAR-X. *IEEE Transactions on Geoscience and Remote Sensing*, in press.
- Habib, A. and Kelley, D., 2001. Single-Photo Resection Using the Modified Hough Transform. In: *Photogrammetric Engineering and Remote Sensing*, Vol. 67(8), pp. 909-914.
- Honikel, M., 1998. Improvement of InSAR DEM accuracy using data and sensor fusion. In: *International Geoscience and Remote Sensing Symposium (IGARSS) 5*, pp. 2348-2350.
- Inglada, J. and Giros, A., 2003. On the possibility of automatic multisensor image registration. *IEEE Transactions on Geoscience and Remote Sensing*, 42(10), pp. 2104-2120.
- Karkee, M., Kusanagi, M., Steward, B.L., 2006. Fusion of Optical and InSAR DEMs: Improving the quality of free data, In: *ASAE Annual Meeting*, Paper number: 061172.
- Mikhail, E., 1993. Linear features for photogrammetric restitution and object completion. Integrating Photogrammetric Techniques with Scene Analysis and Machine Vision, In: *SPIE Proceedings* No. 1944 (Orlando, USA), 16-30.
- Orsomando, F., Lombardo, P., Zavagli, M., Costantini, M., 2007. SAR and Optical Data Fusion for Change Detection, In: *Urban Remote Sensing Joint Event*, pp. 1 – 9.
- Raouf, A. and Lichtenegger, J., 1997. Integrated Use of SAR and Optical Data for Coastal Zone Management. <http://earth.esa.int/workshops/ers97/papers/lichtenegg> (accessed 13 Apr. 2009).
- Sorgel, U., Thiele, A., Cadario, E., Thonnessen U., 2007. Fusion of High-Resolution InSAR Data and optical Imagery in Scenes with Bridges over water for 3D Visualization and Interpretation. In: *Proceedings of Urban Remote Sensing Joint Event 2007 (URBAN2007)*.
- Stamos, A.A., 2007. ThanCad: a 2dimensional CAD for engineers. In: *Proceedings of the Europython2007 Conference*, Vilnius, Lithuania.
- Stamos, A., Vassilaki, D. and Ioannidis, C., 2009. Speed Enhancement of Free-form Curves Matching with Parallel Fortran 2008. In: *1st International Conference on Parallel, Distributed and Grid Computing for Engineering*, Pecs, Hungary.
- Tupin, F., 2006. Fusion of interferometric and optical data for 3D reconstruction. In: *International Geoscience and Remote Sensing Symposium (IGARSS)*, art. no. 4242077, pp. 3627-3630.
- Vassilaki, D., Ioannidis, C., Stamos, A., 2008a. Registration of 2D Free-Form Curves Extracted from High Resolution Imagery using Iterative Closest Point Algorithm. In: *EARSeL's Workshop on Remote Sensing – New Challenges of High Resolution*, Bochum, Germany, pp. 141-152.
- Vassilaki, D., Ioannidis, C., Stamos, A., 2008b. Computation of the closest points for matching curves of different dimensionality. In: *3rd International Conference 'From Scientific Computing to Computational Engineering (SCCE)*, Athens, Greece.
- Vassilaki, D., Ioannidis, C., Stamos, A., 2008c. Geospatial Data Integration using Automatic Global Matching of Free-Form Curves. In: *Digital Earth Summit on Geoinformatics: Tools for Global Change Research*, Potsdam, Germany, pp. 195-200.
- Wang, C.X., Stefanidis, A., Croitoru, A., Agouris, P., 2008. Map Registration of Image Sequences Using Linear Features. In: *Photogrammetric Engineering and Remote Sensing*, Vol. 74(1), pp. 25-38.
- Wegner J., Inglada J., Tison C., 2008. Automatic Fusion of SAR and Optical Imagery based on Line Features. In: *7th European Conference on Synthetic Aperture Radar*, Vol. 1, pp. 171-174.
- Zalmanson, H.G., 2000. Hierarchical Recovery of Exterior Orientation from Parametric and Natural 3-D Curves. In: *International Archives of Photogrammetry and Remote Sensing*, Vol. XXXIII.
- Zhang, Z., 1994. Iterative Point Matching for Registration of Free-form Curves and Surfaces. *International Journal of Computer Vision*, 13(2), pp. 119-152.
- Zitova, B. and Flusser J., 2003. Image registration methods: a survey. *Image and Vision Computing*, 21(11), pp.977-1000.